Published in final edited form as:
J Autoimmun. 2013 February ; 40: 96–110. doi:10.1016/j.jaut.2012.08.004.

A novel regulatory pathway for autoimmune disease: Binding of partial MHC class II constructs to monocytes reduces CD74 expression and induces both specific and bystander T-cell tolerance

Arthur A. Vandenbark[#a,b,c,d,e,*], **Roberto Meza-Romero**[#b,c], **Gil Benedek**[#b,c,d], **Shayne Andrew**[b,c], **Jianya Huan**[c], **Yuan K. Chou**[c,d], **Abigail C. Buenafe**[c], **Rony Dahan**[f], **Yoram Reiter**[f], **Jeffery L. Mooney**[c], **Halina Offner**[b,d,g], and **Gregory G. Burrows**[c,d,h,i]

[a]Research Service, Department of Veterans Affairs Medical Center, Portland, OR 97239, USA

[b]Neuroimmunology Research, Department of Veterans Affairs Medical Center, Portland, OR 97239, USA

[c]Tykeson MS Research Laboratory, UHS-46, 3181 SW Sam Jackson Park Rd, Oregon Health & Science University, Portland, OR 97239, USA

[d]Department of Neurology, Oregon Health & Science University, Portland, OR 97239, USA

[e]Department of Molecular Microbiology & Immunology, Oregon Health & Science University, Portland, OR 97239, USA

[f]Faculty of Biology, Technion-Israel Institute of Technology, Haifa, Israel

[g]Department of Anesthesiology and Perioperative Medicine, Oregon Health & Science University, Portland, OR 97239, USA

[h]Department of Biochemistry, Oregon Health & Science University, Portland, OR 97239, USA

[i]Hematology & Medical Oncology, Knight Cancer Institute, Oregon Health & Science University, Portland, OR 97239, USA

[#] These authors contributed equally to this work.

Abstract

Treatment with partial (p)MHC class II-β1α1 constructs (also referred to as recombinant T-cell receptor ligands – RTL) linked to antigenic peptides can induce T-cell tolerance, inhibit recruitment of inflammatory cells and reverse autoimmune diseases. Here we demonstrate a novel

[*]Corresponding author. Research Service R&D31, Department of Veterans Affairs Medical Center, 3710 SW US Veterans Hosp Rd, Portland, OR 97239, USA. Tel.: +1 503 273 5113; fax: +1 503 721 7975. vandenba@ohsu.edu. .

Conflict of interest Drs. Offner, Burrows, Vandenbark, and OHSU have a significant financial interest in Artielle ImmunoTherapeutics, Inc., a company that may have a commercial interest in the results of this research and technology. This potential conflict of interest has been reviewed and managed by the OHSU and VAMC Conflict of Interest in Research Committees.

Author contributions AAV directed the research and wrote the manuscript; RMR performed the binding assays and identified pMHC binding proteins; GB performed cell staining and evaluated pMHC effects on CD74 expression, MIF signaling and cell migration; SA performed EAE experiments and FACS analysis and prepared the final figures; JH produced and characterized pMHC constructs; YKC performed cell binding studies; ACB performed surface plasmon resonance studies; RD & YR selected and produced the Fab1B11 and FabD2 antibodies used in RTL neutralization studies; JM produced the DR-α1 and DR2-β1 constructs; HO critically reviewed data and edited the manuscript; GGB designed the pMHC constructs, designed experiments and critically reviewed and edited the manuscript.

Appendix A. Supplementary data Supplementary data related to this article can be found at http://dx.doi.org/10.1016/j.jaut.2012.08.004.

regulatory pathway that involves RTL binding to $CD11b^+$ mononuclear cells through a receptor comprised of MHC class II invariant chain (CD74), cell-surface histones and MHC class II itself for treatment of experimental autoimmune encephalomyelitis (EAE). Binding of RTL constructs with CD74 involved a previously unrecognized MHC class II-α1/CD74 interaction that inhibited CD74 expression, blocked activity of its ligand, macrophage migration inhibitory factor, and reduced EAE severity. These findings implicate binding of RTL constructs to CD74 as a key step in both antigen-driven and bystander T-cell tolerance important in treatment of inflammatory diseases.

Keywords

Partial MHC class II; CD74; EAE; MIF

1. Introduction

Myelin-reactive $CD4^+$ T-cells induce experimental autoimmune encephalomyelitis (EAE) and likely contribute to central nervous system (CNS) inflammation, demyelination and axonal damage in multiple sclerosis (MS) [1]. Activation of encephalitogenic T-cells requires presentation of myelin peptides by four-domain MHC class II molecules on antigen presenting cells (APC) in the presence of costimulatory molecules that are needed to prevent induction of T-cell "anergy" [2]. To produce an inhibitory signal for pathogenic TCRs, we created partial MHC class II β1α1 constructs (termed *R*ecombinant *T*-cell receptor *L*igands – RTL) of relevant class II molecules (e.g. DR2 for MS) with covalently tethered myelin peptides [3,4]. These constructs could interact directly with the cognate TCR in the absence of co-stimulatory molecules [5], serving as partial TCR agonists and triggering suboptimal downstream signaling [6,7], cytokine shifts and loss of encephalitogenic activity [8]. RTL treatment of EAE has been established previously in two different strains of DR2-Tg mice, including DR*1501-Tg mice (DRA:DRβ1*1501 strain that develops EAE only after injection of mouse (m)MOG-35-55 peptide [9]) and DR*1502-Tg mice (IE^b:DRβ1*1502 strain that develops EAE after injection of human (h) MOG-35-55 peptide [10]). DR*1501-Tg mice could be treated effectively after disease onset with the cognate mMOG-35-55 peptide tethered to covalently linked β1α1 domains of HLA-DR2 (RTL342M) and DR*1502-Tg mice, with the cognate hMOG-35-55 peptide tethered to the same DR2 β1α1 platform (RTL1000). The potent clinical efficacy of RTLs in mice with EAE led to a successful Phase I trial in multiple sclerosis (MS) using the RTL1000 (pDR2/hMOG-35-55) construct [11,12].

Recent *in vitro* studies demonstrated that RTLs were bound rapidly by myeloid cells and B-cells [13], thus accounting for rapid partitioning from plasma to the cellular compartment (half-life < 10 min) after injection into mice with EAE and subjects with MS [11], and RTL binding to mouse APCs *in vitro* was found to inhibit T-cell activation and transfer of EAE [13]. Taken together, these findings indicated the presence of a cell-associated RTL receptor which initiates peptide-dependent T-cell tolerance involving cell–cell interactions beyond simple ligation of the TCR by soluble RTLs. Our recent detection of immunologically cross-reactive "natural" forms of partial MHC molecules in serum/plasma of both MS and healthy subjects [14] suggests a novel regulatory role for RTL receptors in maintaining homeostasis and inducing T-cell tolerance.

Here we demonstrate binding of RTLs to a molecular complex comprised of CD74, surface histones and MHC class II itself that is expressed predominantly on $CD11b^+$ monocytes and that is required for RTL342M (pDR2/mMOG-35-55) treatment of EAE. RTL constructs with or without tethered antigenic peptide rapidly down-regulated CD74 in a dose-

dependent hierarchical manner, and blocked signaling of the inflammatory cytokine, macrophage migration inhibitory factor (MIF), for which CD74 serves as the primary receptor. Furthermore, a significant structure activity relationship (SAR) was established between RTL-modulated CD74 levels on $CD11b^+$ CNS cells and clinical severity of EAE. These results demonstrate that RTL constructs trigger both peptide-dependent and peptide-independent regulatory pathways that contribute to T-cell tolerance and EAE treatment effects.

2. Materials and methods

2.1. Mice

DR*1501-Tg, DR*1501/GFP-Tg and MBP-TCR/DR2-Tg mice were bred in-house at the Veterinary Medical Unit, Portland Veterans Affairs Medical Center and used at 8e12 weeks of age. All procedures were approved and performed according to institutional guidelines.

2.2. Induction of EAE in DR2-Tg and MBP-TCR/DR2-Tg mice

HLA-DR2 mice were screened by FACS for the expression of the HLA transgenes [5]. HLA-DR2 positive male and female mice between 8 and 12 weeks of age were immunized s.c. at four sites on the flanks with 0.2 ml of an emulsion of 200 μg immunogenic peptide and complete Freund's adjuvant containing 400 μg of heat-killed *Mycobacterium tuberculosis* H37RA (Difco, Detroit, MI) [4,15]. In addition, mice were given pertussis toxin (Ptx) from List Biological Laboratories (Campbell, CA) on days 0 and 2 post-immunization (75 ng and 200 ng per mouse, respectively). Immunized mice were assessed daily for clinical signs of EAE on a 6 point scale of combined hind limb and forelimb paralysis scores. For hind limb scores: 0 = normal; 0.5 = limp tail or mild hind limb weakness (i.e., a mouse cannot resist inversion after a 90° turn of the base of the tail); 1 = limp tail and mild hind limb weakness; 2 = limp tail and moderate hind limb weakness (i.e., an inability of the mouse to rapidly right itself after inversion); 3 = limp tail and moderately severe hind limb weakness (i.e., inability of the mouse to right itself after inversion and clear tilting of hind quarters to either side while walking); 4 = limp tail and severe hind limb weakness (hind feet can move but drag more frequently than face forward); 5 = limp tail and paraplegia (no movement of hind limbs). Front limb paralysis scores are either 0.5 for clear restriction in normal movement or 1 for complete forelimb paralysis. The combined score is the sum of the hind limb score and the forelimb score. Rarely, there is mortality of HLA-DR2 mice with severe EAE and in these cases, mice are scored as a 6 for the remainder of the experiment. Mean EAE scores and standard deviations for mice grouped according to initiation of RTL or vehicle treatment were calculated for each day and summed for the entire experiment (Cumulative Disease Index, CDI, represents total disease load). Daily mean scores were analyzed by a two-tailed Mann Whitney *U* test for nonparametric comparisons between vehicle and pDR2 treatment groups. Mean CDIs were analyzed by a one way ANOVA with Tukey post-test, and a nonparametric one way Kruskal–Wallis ANOVA with Dunn's multiple comparisons post-test to confirm significance between all groups.

2.3. RTL (pMHC) treatment of EAE in DR2-Tg and MBP-TCR/DR2-Tg mice

RTL (pDR2) constructs were injected s.c. daily for 5 days at indicated doses to treat EAE induced in DR*1501-Tg and MBP-TCR/DR2-Tg mice and clinical signs were scored as described above. For neutralization experiments, DR*1501-Tg mice were treated s.c. with vehicle (20 mM Tris–HCl pH 8.0 with 5% w/v D-glucose), 20 μg RTL342M (DR2/mMOG-35–55), 20 μg RTL342M pre-incubated at a 1:1 (40 μg) or 1:2 (80 μg) molar ratio with Fab1B11 (specific for two-domain DR2 constructs) or FabD2 (specific for pDR4/

GAD-555-567 constructs) or Fab1B11 alone in vehicle using a protocol described previously [14].

2.4. Flow cytometry

Analysis of naïve DR2 PBMC subtypes was performed using four-color (fluorescein isothiocyanate, phycoerythrin, propidium iodide, allophycocyanin) flow cytometry. Blood was collected from naïve DR2-Tg mice through cardiac exsanguination into 1XPBS/EDTA. After washing blood in 1XPBS, the red blood cells were lysed with 1× RBC lysis buffer (eBioscience, Inc., San Diego, CA) followed by two washes in RPMI. One million cells were incubated in RPMI with 1 μg unlabeled RTL342M (pDR2/mMOG-35-55) or RTL342H (pDR2/hMOG-35-55) or 1 μg RTL-FITC for 1 h at 37 °C. RTL342M incubation was followed directly by a 30 min incubation at 4 °C with anti-CD3 PE (eBioscience, Inc., San Diego, CA), CD74 PE (Santa Cruz Biotechnology, Inc., Santa Cruz, CA), or CD11b PE, CD11b APC, CD11c APC, and CD19 APC (BD Pharmingen, San Diego, CA). Antibodies and RTLs were thoroughly removed by two additional washes in 1× PBS/0.5% BSA staining medium. Cells were resuspended in staining media containing propidium iodide and immediately analyzed with a FACs Caliber using FCS Express (Los Angeles, CA) software. Data represent 100,000 gated live monocytes and lymphocytes (*in vivo* analyses) or 10,000 gated live monocytes (*in vitro* analyses). For samples assessing Fab neutralization of RTL342M binding and downregulation of CD74, 1 μg RTL was incubated at a 1:1 molar ratio (2 μg) of Fab1B11 or FabD2 for 2 h at room temperature prior to incubation with cells. Upregulation of CD11b staining intensity was evident in all samples that were incubated *in vitro* for 1 h or more, including both controls not incubated with RTL and those that were incubated with RTL-FITC conjugates. In contrast, samples evaluated directly from blood of RTL-injected mice did not show upregulation of CD11b staining intensity. We assume that the changes observed after *in vitro* incubation of $CD11b^+$ cells reflect an activation event triggered by the isolation and/or incubation conditions that were independent of RTL binding.

2.5. Microscopy and live imaging of RTL (pDR2) binding

Two million $CD11b^+$ cells were negatively isolated from DR*1501/GFP-Tg mice by Mouse Monocyte Enrichment Kit and treated with 10 μg/ml RTL342M (pDR2/mMOG-35-55) tagged with Alexa-546 or 50 μg/ml unlabeled RTL342M. The images were acquired on a high resolution wide-field Core DV system (Applied Precision™) utilizing an Olympus IX71 inverted microscope with a proprietary XYZ stage enclosed in a controlled environment chamber: differential interference contrast (DIC) transmitted light and a solid state module for fluorescence. A Nikon Coolsnap ES2 HQ was used to acquire images as optical axis with a 60× (numerical aperture, 1.42) Plan Apo N objective in 2 colors, FITC and TRITC. The pixel size was 0.10704 microns. The images were deconvolved with the appropriate OTF (optical transfer function) using an iterative algorithm of 10 iterations. Histograms were optimized for the most positive image and applied to all the other images for consistency before saving the images as 24 bit merged TIFF. Data were visualized and analyzed using Imaris (Bitplane), and MATLABA (Mathworks).

2.6. Biotinylation of cell surface proteins and cell lysis

Splenocytes from DR*1501-Tg or Class II-KO mice were collected in RPMI and kept in ice before being used in experiments. Cells were washed extensively with cold PBS at pH 8.0 and biotinylated with EZ-Link Sulfo-NHS-LC-Biotin (Pierce Biotechnology, Cat No. 21335) in ice for 15 min to prevent over-labeling. The reaction was quenched by diluting the biotinylated cell suspension 5× with TEN (50 mM Tris, 2 mM EDTA, 150 mM NaCl) buffer at pH 7.4. Subsequent washes were carried out with TEN buffer to remove the biotinylation reagent and the pellet was kept frozen until lysis. Cell pellets were thawed in ice and lysis

was performed in TEN buffer containing 1% Triton X-100 (TEN-TX100) or 1% CHAPS (TEN-CHAPS) for 30–60 min in the presence of protease inhibitors (Halt Protease Inhibitor Cocktail, Pierce Biotechnology) in addition to 1 μM PMSF (Sigma). After lysis, samples were cleared by centrifugation at 14,000 rpm for 15 min at 4 °C and the supernatant was collected for further analysis.

2.7. Direct and competitive binding assays on whole cells

In order to determine whether a potential saturable, specific binding site(s) was present on the cell surface of splenocytes, two million cells from DR*1501-Tg mice were incubated with increasing concentrations (up to 400 nM) of AlexaFluor488-labeled RTL1000 in RPMI for 1 h in ice (to minimize internalization through phagocytic mechanisms) and then cells were lysed in 100 μl 6 M urea to dissociate and solubilize bound labeled ligand for subsequent analysis. The lysate was centrifuged to remove insoluble material (nuclei, organelles), the supernatant separated by SDS electrophoresis in a 10–20% PAGE and the gel scanned for AlexaFluor488 to visualize labeled RTL. Band intensity was quantified by densitometry using the Quantity One Software (Biorad) and plotted vs. the labeled RTL1000 concentration. Data were analyzed using Prism Software and fit to 1- or 2-binding site mathematical models. Competitive binding was carried out using 2 million splenocytes and a constant concentration of AlexaFluor488-labeled RTL1000 (280 nM) in the presence of increasing concentrations of unlabeled RTL constructs (0–8 μM). Afterwards, cells were washed, lysed and analyzed in a similar way as described above for saturation assays in whole cells. Results are presented as EC_{50}, the concentration of the competitor required to compete for half of the specific binding.

2.8. Immunoprecipitation and direct and competitive binding assays for CD74 and MHC class II molecules

For immunoprecipitation experiments, antibody TU39 (BD Pharmingen) was pre-bound to bead-conjugated Protein A for 2 h in ice-cold TEN-TX100 or TEN-CHAPS followed by RTL binding to these complexes. Lysate (previously pre-cleared with bead-conjugated Protein A) was added to the tube and binding was carried out overnight at 4 °C with soft orbital shaking. Samples were extensively washed with TEN buffer and the appropriate detergent. For CD74 immunoprecipitation, ln-1 mAb was adsorbed to bead-conjugated Protein L as described above and pre-cleared lysate was added to this mixture. When necessary, bound material was eluted by boiling the immune complexes in electrophoresis sample buffer and analyzed by SDS-PAGE and Western blot.

For direct binding of RTL constructs, Protein-L/ln-1/CD74 complexes were prepared as described above. For these experiments, labeled ligand constructs were incubated for 4 h at 4 °C in 1% CHAPS in TEN buffer and free ligand was removed by extensive washing. Elution of bound proteins was carried out as described before and analyzed by SDS-PAGE. Likewise, competition experiments were carried out using a 2:1 molar ratio of labeled RTL1000 (pDR2/hMOG-35-55) to “cold” competitor in a 500 μl reaction volume at 4 °C for 3–4 h in TEN-CHAPS buffer. A competition experiment between RTL1000 and DR-α1 domain for the binding to CD74 was done by using 0.160 nmol (4 μg) of labeled RTL1000 and increasing concentrations (0, 0.032, 0.096, 0.320, and 0.960 nmol) of the DR-α1 domain in a total reaction volume of 0.5 ml. Under these conditions the final concentration of RTL1000 was 320 nM. In all assays involving fluorescent labeling, the chromophore was detected by scanning at the appropriate wavelength using a Molecular Imager FX (Bio-Rad) and the fluorescence intensity was determined using Quantity One (Bio-Rad), the software associated with the equipment.

In order to test ligand binding to the separate components of the RTL receptor, DR*1501-Tg splenocytes were biotinylated and lysed as described above and CD74 was immunoprecipitated overnight at 4 °C with ln-1 monoclonal antibody. Immune complexes (Protein L-beads/ln-1/CD74) were analyzed for their ability to bind FITC-labeled RTL constructs by performing a direct binding saturation with increasing concentrations of the different constructs (0–10 nM). Binding was carried out for 4 h at 4 °C with gentle shaking and in the presence of 1% CHAPS in TEN buffer. Afterwards, the complexes were washed thoroughly with 1% CHAPS/TEN and once with only TEN buffer to remove excess detergent. Bound proteins were eluted in 2% SDS electrophoresis sample buffer at 90 °C for 6–8 min and beads were sedimented. After the supernatant was collected and proteins separated using 10–20% SDS-PAGE, the gel was scanned for FITC chromophore and quantified by densitometry. Ligand concentration was plotted vs. the fluorescence intensity of the bands and the curve generated was fit to one or two binding sites with the Prism Software. Likewise, MHC class II from DR*1501-Tg mice was purified with L243 monoclonal antibody conjugated to Protein-L/beads using the CD74-depleted lysate. Under these conditions a homogeneous preparation of MHC class II from DR*1501-Tg mice was isolated. Direct binding of MHC class II to saturating concentrations of the RTL constructs was carried out and analyzed as described above.

2.9. Electrophoresis, Western blotting and LC/MS/MS

After elution from immunoprecipitates, proteins were separated using 10–20% SDS-PAGE and visualized by Coomassie Blue staining, or they were blotted to PVDF and detected with streptavidinconjugated PE. Relevant proteins detected by PE staining were localized in a replica gel stained with Coomassie Blue, the gel bands were cut, digested with trypsin and characterized by LC-MS/MS.

2.10. RTL342M (pDR2/mMOG-35-55) inhibition of MIF-enhanced expression of ICAM-1

Splenocytes were isolated from DR*1501 Tg mice and cultured in the presence or absence of 10 μg/ml RTL342M (pDR2/mMOG-35-55) in complete RPMI medium 1640 with 2% heat inactivated FCS at 37 °C in 5% CO_2 for 1 h. Cells were stimulated with 10 ng/ml LPS (*Escherichia coli*, serotype 055:B5, Sigma–Aldrich) and 100 ng/ml recombinant MIF (R&D systems, Minneapolis, MN, USA) for 1 h before harvesting. Total RNA was isolated from splenocytes using an RNeasy cultured cell kit according to the manufacturer's instructions, which included a DNase step. (Qiagen, Valencia, CA, USA). Quantitative real time PCR was performed using the ABI7000 sequence detection system with gene-on-demand assay products (Applied Biosystems) for ICAM-1 (Assay ID: Mm00516023_m1). GADPH housekeeping gene was amplified as an endogenous control. Primers were used according to manufacturer's instructions.

3. Results

3.1. RTLs (pDR2/MOG-35-55) bind predominantly to CD11b$^+$ monocytes

Although our previous studies indicated that pMHC constructs could bind to monocytes, B-cells, DC and platelets, only RTL-armed monocytes inhibited T-cell activation and transfer of EAE [13]. To determine if these *in vitro* binding experiments reflected RTL binding *in vivo*, naïve DR*1501-Tg mice were injected i.v. with RTL342M (pDR2/mMOG-35-55)-FITC or RTL1000 (pDR2/hMOG-35-55)-FITC, and viable PBMC subtypes were evaluated for RTL binding in the monocyte gate (Fig. 1a). The major RTL-binding cell population detected *ex vivo* indeed was CD11b$^+$ monocytes, with only modest binding by B-cells, T-cells and DC (Fig. 1b). Only minimal RTL binding of these respective PBMC subpopulations was detected in the lymphocyte gate (Supplemental Fig. 1a). This pattern of cell binding by both RTL342M and RTL1000 was validated *in vitro* after 1 h incubation

with PBMC from DR*1501-Tg mice (Fig. 1c and Supplemental Fig. 1b), thus demonstrating equivalency of these two closely related pMHC constructs that differ only by a single amino acid residue in the tethered MOG peptide (S42 vs. P42, respectively). Direct binding of labeled RTL342M (pDR2/mMOG-35-55) to GFP^+CD11b^+ monocytes, visualized by color enhanced fluorescence microscopy (Fig. 1d and Supplemental Movie), demonstrated cell surface as well as likely-internalized complexes of RTL, strongly suggesting binding to RTL receptors.

Supplementary video related to this article can be found at http://dx.doi.org/10.1016/j.jaut.2012.08.004.

3.2. Binding of RTL1000 (pDR2/hMOG-35-55) to $DR2^+$ splenocytes involves two binding sites with different relative affinities

To characterize the pMHC receptor on $DR2^+$ splenocytes, a saturation binding curve was established using 2 million spleen cells incubated for 1 h on ice (to inhibit phagocytosis and low affinity non-specific binding) with increasing concentrations of Alexa-488-labeled RTL1000 (pDR2/hMOG-35-55), followed by extensive washing. Cells with captured RTL1000 were centrifuged and the cell pellet solubilized in 6 M urea, with protein components separated by SDS-PAGE and fluorescence intensity of extracted Alexa-488-labeled RTL1000 quantified after gel electrophoresis. As is shown in Fig. 2a, the saturation data best fit a hyperbolic two-site binding curve ($R^2 = 0.998$), with the first binding site for RTL1000 showing high affinity binding and rapid saturation with a K_D of 2.65 nM and the second binding site showing lower affinity binding for RTL1000 with a K_D of 131 nM.

Competition experiments were then performed in which mixtures of Alexa488-labeled RTL1000 in combination with increasing concentrations of unlabeled RTL1000 were incubated with spleen cells. Similar to the saturation experiments described above, the competition experiments demonstrated a two-site binding pattern for DR*1501-Tg splenocytes (Fig. 2b). The lower affinity Site 2 had an EC50 of 11 nM, indicating that a relatively low concentration of unlabeled RTL was needed to displace labeled RTL1000 (Fig. 2d). In contrast, the higher affinity Site 2 had an EC50 of 4000 nM, indicating that a much higher (>350-fold) concentration of unlabeled RTL was needed to displace labeled RTL1000 (Fig. 2d). Taken together, these data clearly demonstrate the presence of two independent RTL receptors or a receptor complex on DR*1501-Tg splenocytes that involves at least two distinct binding affinities.

3.3. Different receptor affinities for the β1α1 vs. peptide moieties

Additional competition studies were performed using Alexa-488-labeled RTL1000 (pDR2/hMOG-35-55) mixed with increasing concentrations of other RTL constructs to evaluate the binding of both the MHC class II β1α1 and peptide moieties of pDR2/peptide. Although RTL1000 (pDR2/hMOG-35-55), RTL342M (pDR2/mMOG-35-55) and RTL340 (pDR2/MBP-85-99) all could compete for both Site 1 and Site 2 (Fig. 2b & 2d), “empty” RTL302-5D (pDR2/no peptide) could compete with RTL1000 only for the lower affinity Site 2. These data clearly indicate that the lower affinity binding site for RTL interacts with the β1α1 moiety even in the absence of a covalently-tethered peptide, whereas the higher affinity binding site required presence of the covalently-tethered antigenic peptide moiety.

3.4. MHC class II is required for the high affinity binding site for RTL1000

To evaluate the contribution of MHC class II to RTL binding, competition studies were performed using splenocytes from MHC class II deficient mice. As is shown in Fig. 2c & d, only a single low affinity binding site was present on MHC class II-KO splenocytes. These results implicated cell surface expressed MHC class II itself as the high affinity binding site

for RTL, likely involving interaction of the tethered antigenic peptide with the MHC class II binding cleft.

3.5. Identity of RTL binding components on the surface of DR*1501-Tg splenocytes

To identify RTL-binding proteins, TU39 monoclonal antibody alone or TU39-bound RTL1000 conjugated to Protein A was incubated overnight with biotinylated whole splenocytes in 1% CHAPS buffer. Bound membrane proteins were eluted and analyzed by electrophoresis and Western blotting after visualization with streptavidin-PE (to detect biotinylated membrane proteins) in the absence or additional presence of anti-DR mAb (HK14) to detect RTL1000. This analysis revealed at least four distinct bands in addition to RTL1000 that were either enriched (15 kD and 18 kD) or could not be detected unless RTL1000 was present (31 kD and 72 kD) (Fig. 2e). Elution of parallel bands from an unstained sample and sequencing by LC-MS/MS (Supplementary Fig. 2) identified the major RTL-binding proteins as H4 histone (14 kD), H2A, H2B and H3 histones (18 kD), CD74 (31 kD) and MHC class II (72 kD). The 72 kD class II sequence was from the H-2Eα2 domain that was derived from the expressed DR2-transgene [16] and not from the RTL1000 construct. Further evaluations using plasmon surface resonance measurements confirmed low affinity binding interaction between RTL1000 and the histone complex (Supplemental Fig. 3).

3.6. RTL DR-α1 domain binds to CD74 but not to MHC class II

The potential binding of RTL constructs to CD74 has important immunoregulatory implications for antigen presentation, autoimmune diseases and cancer [17,18]. To confirm involvement of CD74 as a major component of the RTL receptor, CD74 was immunoprecipitated from biotinylated DR*1501-Tg splenocyte membrane preparations using Protein-L-conjugated anti-CD74 ln-1 mAb and visualized with streptavidin-PE (Fig. 3a). The ln-1 mAb-immunoprecipitated CD74 pulled down p72 and p130 proteins in addition to p31 and p41, and did not co-precipitate full-length MHC class II molecules (Fig. 3a). Moreover, after incubating FITC-labeled RTL with bead-immunopurified CD74, both RTL1000 (pDR2/hMOG-35-55) and RTL342M (pDR2/mMOG-35-55) were bound abundantly by CD74 (Fig. 3b), whereas RTL340 (pDR2/MBP-85-99) and “empty” RTL302-5D were detected at much lower levels under the same conditions. The moiety of RTL that binds CD74 was further determined to be the DR-α1 but not the DR2-β1 domain, as shown by direct binding experiments (Fig. 3b) and competitive binding studies (Supplemental Fig. 4a) that established a single binding site on CD74 for the DR-α1 domain of RTL1000 (Supplemental Fig. 4b).

Further direct binding of increasing concentrations of FITC-labeled RTL constructs to immunopurified CD74 (Fig. 3c) confirmed CD74 binding of RTL1000, RTL342M and DR-α1 (but not other RTL constructs) and established that binding was dose-dependent, saturable and involved a single binding site in the low nM range (2.9–4.5 nM, Supplemental Fig. 5). In contrast, binding of FITC-labeled RTL constructs to four-domain MHC class II molecules (Fig. 3d) in the same membrane preparation (after CD74-depletion) established binding of RTL1000 and RTL342M, but not DR-α1 or other pDR2 constructs, that was dose-dependent, saturable and that also involved a single binding site in the low nM range (1.1–2.0 nM, Supplemental Fig. 5).

These data strongly support the presence of a single relatively high affinity binding site on CD74 for a determinant in the DR-α1 moiety of the RTL molecule and a separate, slightly higher affinity binding site on 4-domain class II for an RTL determinant not present on the DR-α1 domain that could possibly include the covalently-tethered peptide itself or a

conformational epitope on the DR2-β1α1 moiety that requires the presence of a covalentlytethered antigenic peptide.

3.7. Reduced CD74 expression after RTL binding to monocytes

Because of the known involvement of CD74 and CLIP (Class II-associated invariant chain peptide) in MHC class II peptide loading and tolerance induction, we characterized the effects of RTL treatment on CD74 expression in $CD11b^+$ monocytes. *Ex vivo* studies demonstrated that expression of CD74 on $CD11b^+$ monocytes was increased during EAE (Fig. 4a). Moreover, treatment of EAE mice with RTL342M (pDR2/mMOG-35-55) at onset of clinical signs produced a significant down-regulation of CD74 cell-surface expression within 48 h on $CD11b^+$ cells evaluated from blood, spleen and spinal cords (Fig. 4b & c), but did not alter MHC class II cell surface expression (blood: 13% vs. 11%, p = NS; spleen: 22% vs. 20%, p = NS; RTL342M treated vs. vehicle treated, respectively) that predominantly is not associated with CD74 on the monocyte cell surface [19,20]. The downregulation of CD74 expression was not due to the blocking of the anti-CD74 Ab binding site by RTL, since CD74 could be immunoprecipitated from biotinylated DR*1501-Tg splenocyte membrane preparations that were preincubated with RTL342M or DR-α1, using Protein-L-conjugated anti-CD74 ln-1 mAb (Supplemental Fig. 7).

3.8. CD74 expression correlates inversely with RTL binding to monocytes

To explore the relationship between binding of RTL and expression of CD74, $CD11b^+$ monocytes were incubated with increasing concentrations of RTL constructs for 1 h at 37 °C and then evaluated by FACS for RTL capture and cell-surface expression of CD74, as shown for RTL1000 (Fig. 4d). Results from five different constructs (Fig. 4e) demonstrated decreased cell-surface expression of CD74 as a function of increasing RTL binding, a relationship that was shown to be highly significant when data points for all constructs were combined ($p < 0.001$, Fig. 4e lower right panel).

3.9. Fab blockade of RTL342M downregulation of CD74 on monocytes neutralizes RTL treatment effects on EAE

To determine if RTL342M downregulation of CD74 on monocytes was necessary for treatment of EAE, Fab1B11 selected for binding to 2-domain DR2 molecules and a control, FabD2, reactive to a DR4/GAD-555-567 RTL construct [14] were evaluated for their respective abilities to block RTL-induced downregulation of CD74 expression and thus neutralize RTL treatment effects. Incubation of RTL342M (pDR2/mMOG-35-55) with Fab1B11 but not FabD2 at a 1:1 or 1:2 molar ratio for 2 h resulted in a significant (~60%) blockade of RTL342M-induced downregulation of CD74 expression on $CD11b^+$ monocytes *in vitro* ($p < 0.01$, Fig. 5a) and comparable (~60%) neutralization of the protective activity of RTL342M *in vivo* after 3 daily s.c. injections into mice with EAE ($p < 0.0001$, Fig. 5b). In a related study, 5 daily injections of free mMOG-35-55 peptide at an equimolar concentration as RTL342M (10 μg vs. 100 μg, respectively) did not produce significant inhibition of EAE compared to RTL342M (Supplemental Fig. 6), thus confirming that the inhibitory activity was not mediated by the MOG peptide and that the neutralizing effect of Fab1B11 was directed against the DR2-β1α1 moiety rather than mMOG-35-55. These combined selective effects of Fab1B11 vs. FabD2 demonstrate that RTL binding and downregulation of CD74 is necessary for its therapeutic activity on EAE.

3.10. RTL binding inhibits MIF-induced signaling and increases random migration of $CD11b^+$ monocytes

To establish if RTL binding directly inhibited MIF-induced signaling, naïve splenocytes were incubated with RTL342M (pDR2/mMOG-35-55) for 1 h prior to stimulation with MIF

and LPS [21] and then evaluated for expression of ICAM-1 [22]. As is shown in Fig. 6a, RTL342M significantly reduced MIF-enhanced induction of ICAM-1 message to LPS background levels, demonstrating complete inhibition of the MIF-dependent effects but no further effect on LPS-dependent activation.

Binding of MIF to CD74 is known to inhibit random migration of macrophages [23]. To determine if reduced CD74 cell-surface expression mediated by RTL342M binding altered the migration pattern of monocytes, movement of GFP^+CD11b^+ cells isolated from naïve DR*1501/GFP-Tg mice was tracked for 2 h *in vitro* with or without added RTL342M using live imaging microscopy. As is shown in Fig. 6b–d significant increases were observed in measured speed ($p < 0.0005$, Fig. 6b), mean square displacement ($p < 0.0005$, Fig. 6c) and random migration path (Fig. 6d and Supplemental Movie) in the presence of RTL342M. These data demonstrate that reduced cell surface expression of CD74 induced by RTL is associated with reduced expression of ICAM-1 and increased random migration of $CD11b^+$ monocytes, consistent with the blockade of MIF effects.

3.11. RTL constructs can inhibit EAE in an antigenic peptide-independent manner

The data presented above demonstrated remarkable differences in the ability of various RTL constructs to modulate cell surface expression levels of CD74, (RTL342M ~ RTL1000 >> RTL340 > DR-α1 ~ RTL302-5D), suggesting a hierarchy of clinical efficacy mediated through CD74 modulation. This would predict that RTL constructs with the best binding and CD74-modulating properties at standard treatment concentrations (100 μg RTL daily × 5) might have inhibitory effects on EAE when tethered to mismatched, noncognate peptides or even without bound peptides, in a manner commensurate to their respective effects on CD74 expression. Thus, RTL constructs with tethered hMOG-35-55 or mMOG-35-55 were compared with RTL340 (DR2/MBP-85-99), RTL302-5D (pDR2/no peptide) or vehicle alone for treatment of EAE induced with MBP-85-99 peptide/CFA/Ptx in MBP-TCR/DR2-Tg mice. As is shown in Fig. 7a, both RTL1000 (DR2/hMOG-35-55) and RTL342M (DR2/mMOG-35-55 – more potent modulation of CD74 but bearing noncognate peptides) provided a treatment effect on EAE comparable to that of RTL340 (DR2/MBP-85-99 bearing the cognate peptide but with less potent modulation of CD74), thus satisfying the prediction. In contrast, “empty” RTL302-5D (DR2/no peptide) was still ineffective at treating EAE using the standard treatment paradigm as expected (no bound peptide and weak modulating effects on CD74 expression).

To explore further the possible peptide-independent inhibitory effects of RTL constructs on EAE, a 10-fold-higher dose of RTL302-5D (DR2/no peptide given at 1 mg × 2 or 5 days), which showed significant binding and modulation of CD74 (Fig. 4e), was tested for therapeutic activity in DR*1501-Tg mice with mMOG-35-55-induced EAE compared to the standard dose and treatment regimen (100 μg × 5) of “empty” RTL302-5D, RTL342M and vehicle. As shown in Fig. 7b, treatment of EAE with the 1 mg dose of “empty” RTL302-5D indeed resulted in significant reduction of daily and cumulative EAE scores compared to treatment with vehicle or 100 μg RTL302-5D. Moreover, treatment with the standard dose of RTL342M (pDR2/mMOG-35-55) daily for 2 or 5 days resulted in even more potent inhibition of EAE than 1 mg RTL302-5D. These results demonstrate conclusively an antigenic peptide-independent treatment effect of the “empty” RTL302-5D construct on EAE that is potentiated by inclusion of the cognate peptide within the RTL342M construct.

3.12. Structure–activity relationship (SAR) of RTL modulation of CD74 and EAE severity

To more formally establish an SAR between RTL modulation of CD74 and EAE severity, CD74 levels were assessed on CNS-derived $CD11b^+$ cells from naïve DR*1501-Tg mice (background levels of CD74 with no clinical EAE) and mMOG-35-55 immunized

DR*1501-Tg mice treated with RTL342M (DR2/mMOG-35-55, 100 μg daily × 2), "empty" RTL302-5D (1 mg × 2) or vehicle (maximal disease-induced levels of CD74 with no treatment effect) 15 days after induction of EAE. As is shown in Fig. 7c, there was a significant relationship ($p = 0.035$) between CD74 levels on $CD11b^+$ cells and the average CDI for the different groups of mice, thus providing strong support for the SAR. To further demonstrate the relationship between the binding and downregulation of CD74 and reduction of EAE severity by RTL constructs, $CD11b^+$ monocytes were incubated with the DR2-β1 construct, which does not bind CD74 (Fig. 3b), for 1 h at 37 °C and then evaluated by FACS for cell-surface expression of CD74. The DR2-β1 construct did not downregulate CD74 levels on $CD11b^+$ monocytes and as expected, did not treat EAE (Supplemental Fig. 8).

4. Discussion

Peptide-loaded, APC-associated MHC class II molecules confer specificity for TCR-mediated activation of $CD4^+$ T-cells. However, little is known about MHC class II catabolic pathways and biological activities of MHC class II fragments. We here demonstrate that binding of RTL constructs to a previously unrecognized receptor on $CD11b^+$ monocytes downregulates expression of CD74 and directly inhibits MIF activity. These initial events not only mediate potent peptide-independent inhibition of MIF signaling, but also trigger downstream inhibition of peptide-dependent T-cell activation, resulting in reduced infiltration of inflammatory cells into the CNS and reversal of EAE [24–26]. Cell binding of RTL constructs involved both relatively high and low affinity interactions with the surface receptor that was required for EAE treatment. Further analysis revealed a minimum of three RTL receptor components, including CD74, MHC class II and assembled cell surface histone nucleosomes [27–29] that bound RTL with low affinity.

The major new finding of this study is the dose-dependent binding and down-regulation of cell-surface CD74 on monocytes by a hierarchy of RTL constructs, the most active being RTL1000 (DR2/hMOG-35-55) and RTL342M (DR2/mMOG-35-55) that possess potent activity for treating MOG-35-55 peptide-induced EAE. In contrast, RTL340 (DR2/MBP-85-99) was much less efficient at binding and down regulating CD74 under standard conditions, but retained the ability to effectively treat EAE in MBP-TCR/DR2-Tg mice, likely through an MBP peptide-specific T-cell tolerance mechanism. Thus, the RTL342M (DR2/mMOG-35-55) and RTL340 (DR2/MBP-85-99) constructs have comparable therapeutic activity when treating EAE induced with their cognate encephalitogenic peptides. However, RTL constructs containing MOG-35-55 peptides differ from RTL340 containing MBP-85-99 in their remarkable ability to treat EAE induced by non-cognate encephalitogenic peptides. That is, whereas RTL340 could not treat mice with MOG peptide-induced EAE, both RTL342M and RTL1000 constructs could fully treat mice with MBP peptide-induced EAE.

These treatment effects on EAE of different RTL constructs were directly related to their ability to down-regulate CD74. Indeed, 10-fold higher doses of the "empty" RTL302-5D that also possessed the ability to down-regulate CD74 produced a significant *peptide-independent* treatment effect on mMOG-35-55 induced EAE. Moreover, incubation with Fab1B11 specific for two-domain DR2-RTL constructs neutralized RTL-induced downregulation of CD74 and EAE treatment effects. Subsequent comparisons established a significant structure–activity relationship (SAR) between CD74 levels on CNS-derived $CD11b^+$ cells and EAE severity which clearly established RTL342M as the most effective construct and predicted dose-dependent therapeutic activity of other constructs commensurate with their ability to modulate CD74 levels. The SAR is further supported by the lack of an EAE treatment effect of the DR2-β1 construct, which does not bind to CD74

or downregulate its expression levels. Such previously unrecognized binding interactions between RTL and CD74 constitute a novel form of “bystander” suppression that may act alone or in tandem with peptide-dependent induction of T-cell tolerance shown previously using various mouse and human RTL constructs. The potent antigen-independent inhibition of CD74 levels by DR2/MOG-35-55 RTL constructs not only provides a cogent explanation for the successful treatment of experimental stroke [30], in which the specificities of the infiltrating inflammatory T-cells have not yet been established, but also establishes RTL1000 (DR2/hMOG-35-55) as the optimal construct to treat MS that certainly involves multiple encephalitogenic T-cell specificities. It is important to note that our preliminary data demonstrate strong RTL1000 binding to human monocytes and down-regulation of CD74 expression that occurs in an essentially identical manner as observed for mouse monocytes (Benedek et al. manuscript in preparation).

Binding interactions of RTL with MHC class II and CD74 are likely to be highly interactive due to the essential role of CD74 (invariant chain = Ii) in chaperoning newly synthesized MHC class II through the endocytic pathway to the cell surface of APC [31]. CD74 is a type II transmembrane glycoprotein containing a trimerization domain flanked by two highly unstructured regions [32]. Earlier models suggested that the homotrimeric structure could bind up to three αβ MHC class II heterodimers to form a nonameric complex, $Ii_3(\alpha\beta)_3$ [33,34]. More recent models propose a pentameric complex, with the Ii homotrimer chaperoning a single MHC class II heterodimer from the ER [35]. While the structure of MHC class II bound to CD74 has not yet been solved, interactions between CD74 and the αβ MHC class II heterodimer have been mapped to at least three discrete extracellular locations and the transmembrane domains [36–39].

Our studies demonstrated direct single-site, relatively high affinity competitive binding of DR2/MOG-35-55 RTL constructs and the DR-α1 domain to CD74. In contrast, we found single-site, relatively higher affinity binding of DR2/MOG-35-55 RTL constructs but not DR-α1 to MHC class II, possibly implicating the covalently tethered MOG-35-55 peptide itself or a peptide-dependent conformation of the DR2-β1α1 moiety as the MHC class II binding determinant. Such binding of tethered MOG-35-55 peptide to cell-associated 4-domain class II potentially could allow the “empty” cleft of the β1α1 moiety to bind the remaining CLIP-region peptides in the CD74 trimer. Future studies will identify the DR-α1 residues that interact with CD74 and determine if the CLIP region of CD74 binds directly to the β1α1 peptide-binding groove. These possible molecular interactions within the pMHC receptor complex are predicted by our two-site binding data, and are further supported by the requirement of MHC class II for optimal RTL binding to CD74.

Our results strongly suggest that the affinity of the tethered peptide for the DR2 RTL β1α1 binding groove likely influences the interaction of the construct with CD74, with the higher affinity peptides (e.g. MOG-35-55) facilitating CD74 binding by RTLs better than the lower affinity peptides (e.g. MBP-85-99). β1α1 constructs that do not have a tethered peptide also have decreased binding affinity for CD74, suggesting that the tethered peptide, presumably in the binding groove, stabilizes the CD74 interaction. Alternatively, the tethered higher affinity peptides may have similar or relatively stronger affinity for the binding groove of cell-associated 4-domain class II (data in Fig. 2c support loss of the higher affinity interaction in class II knockout mice) than for the 2-domain constructs, thus producing conformational changes in the two-domain structures that could facilitate binding to CD74.

Down-regulation of CD74 by RTL constructs has important regulatory implications. CD74 in combination with CD44, CXCR2 & CXCR4 [40,41] is the receptor for MIF [42,43] that inhibits random migration of monocytes [23] and promotes severity and progression of EAE [44,45]. Modulation of MIF is known to inhibit downstream effects on VCAM-dependent

homing of encephalitogenic T-cells to the CNS [45], expression of ICAM-1 and VLA-4 [46,47] and formation of the immunological synapse between T-cells and APC [48,49], which in turn could affect peptide-dependent T-cell proliferation and cytokine release [13,25]. Moreover, RTL down-regulation of CD74 may result in internalization and re-expression of MHC class II/CLIP, which may promote T-cell tolerance as a null agonist [50]. Our study demonstrates that down-regulation of CD74 cell surface expression on monocytes after RTL342M binding results in direct inhibition of MIF-induced enhancement of ICAM-1 expression and increased random migration. These findings suggest that the SAR between CD74 expression and EAE severity involves decreased expression of ICAM-1 and increased random migration of monocytes, which could affect both their chemotaxis to the CNS and their interaction with pathogenic T cells.

5. Conclusions

In summary, we have implicated binding and down-regulation of CD74 on monocytes as an essential early event in RTL treatment of EAE that involves regulation of both peptide-specific and bystander T-cells. RTL342M treatment of EAE resulted in reduced levels of CD74 on CNS-derived $CD11b^+$ cells both at early (48 h) and later (15 days) time points, suggesting assessment of CD74 levels as an *ex vivo* biomarker for disease activity as well as efficacy of RTL constructs. This novel regulatory pathway may also be triggered by natural partial MHC structures detected in human serum and plasma that could represent a dominant homeostatic mechanism for terminating inflammatory responses, maintaining T-cell tolerance and preventing autoimmune diseases.

Supplementary Material

Refer to Web version on PubMed Central for supplementary material.

Acknowledgments

The authors wish to thank Dr. Peter McWilliams for suggestions regarding data presentation, Ms. Eva Niehaus for assistance in preparing the manuscript and Aurelie Snyder and the Advanced Light Microscopy Core at The Jungers Center, OHSU, for technical assistance.

This work was supported by NIH grants NS47661, AI43960, DK0688861 and NS41965 and National Multiple Sclerosis Society grant RG3794-B-6. This material is based upon work supported in part by the Department of Veterans Affairs, Veterans Health Administration, Office of Research and Development, Biomedical Laboratory Research and Development. The contents do not represent the views of the Department of Veterans Affairs or the United States Government.

References

[1]. Steinman L. Multiple sclerosis: a two stage disease. Nat Immunol. 2001; 2:762–5. [PubMed: 11526378]

[2]. Jenkins MK, Schwartz RH. Antigen presentation by chemically modified splenocytes induces antigen-specific T cell unresponsiveness *in vitro* and *in vivo*. J Exp Med. 1987; 165:302. [PubMed: 3029267]

[3]. Burrows GG, Adlard KL, Bebo BF Jr, Chang JW, Tenditnyy K, Vandenbark AA, et al. Regulation of encephalitogenic T cells with recombinant TCR ligands. J Immunol. 2000; 164:6366–71. [PubMed: 10843691]

[4]. Vandenbark AA, Rich C, Mooney J, Zamora A, Wang C, Huan J, et al. Recombinant TCR ligand induces tolerance to MOG-35-55 peptide and reverses clinical and histological signs of chronic experimental autoimmune encephalomyelitis in HLA-DR2 transgenic mice. J Immunol. 2003; 171:127–33. [PubMed: 12816990]

[5]. McMahan RH, Watson L, Meza-Romero R, Burrows GG, Bourdette DN, Buenafe AC. Production, characterization, and immunogenicity of a soluble rat single chain T cell receptor specific for an encephalitogenic peptide. J Biol Chem. 2003; 278:30961–70. [PubMed: 12773544]

[6]. Burrows GG, Chou YK, Wang C, Chang JW, Finn TP, Culbertson NE, et al. Rudimentary TCR signaling triggers default IL-10 secretion by human Th1 cells. J Immunol. 2001; 167:4386–95. [PubMed: 11591763]

[7]. Wang C, Mooney JL, Meza-Romero R, Chou YK, Huan J, Vandenbark AA, et al. Recombinant TCR ligand induces early TCR signaling and a unique pattern of downstream activation. J Immunol. 2003; 171:1934–40. [PubMed: 12902496]

[8]. Burrows GG. Systemic immunomodulation of autoimmune disease using MHC-derived recombinant TCR ligands. Curr Drug Targets Inflamm Allergy. 2005; 4:185–93. [PubMed: 15853741]

[9]. Link JM, Rich CM, Korat M, Burrows GG, Offner H, Vandenbark AA. Monomeric DR2/MOG-35-55 recombinant TCR ligand treats relapses of experimental encephalomyelitis in DR2 transgenic mice. Clin Immunol. 2007; 123:95–104. [PubMed: 17257899]

[10]. Chou YK, Culbertson N, Rich C, LaTocha D, Huan J, Link J, et al. T cell hybridoma specific for myelin oligodendrocyte glycoprotein 35-55 peptide produced from HLA-DRB1*1501 transgenic mice. J Neurosci Res. 2004; 77:670–80. [PubMed: 15352213]

[11]. Yadav V, Bourdette DN, Bowen JD, Lynch SG, Mattson D, Peiningerova J, et al. Recombinant T-cell receptor ligand (RTL) for treatment of multiple sclerosis: a double-blind, placebo-controlled, phase 1, dose-escalation study. Autoimmune Dis. 2012; 2012:1–11.

[12]. Offner H, Sinha S, Burrows GG, Ferro AJ, Vandenbark AA. RTL therapy for multiple sclerosis: a phase I clinical study. J Neuroimmunol. 2011; 231:7–14. [PubMed: 20965577]

[13]. Sinha S, Miller LM, Subramanian S, McCarty OJT, Proctor T, Meza-Romero R, et al. Binding of recombinant T cell receptor ligands (RTL) to antigen presenting cells prevents upregulation of CD11b and inhibits T cell activation and transfer of experimental autoimmune encephalomyelitis. J Neuroimmunol. 2010; 225:52–61. [PubMed: 20546940]

[14]. Dahan R, Tabul M, Chou YK, Meza-Romero R, Andrew S, Ferro AJ, et al. TCR-like antibodies distinguish conformational and functional differences in two-versus four-domain auto reactive MHC class II-peptide complexes. Eur J Immunol. 2011; 41:1465–79. [PubMed: 21469129]

[15]. Buenafe AC, Andrew S, Afentoulis M, Offner H, Vandenbark AA. Prevention and treatment of experimental autoimmune encephalomyelitis with clonotypic CDR3 peptides: CD4+FoxP3+ expansion T-regulatory cells suppress interleukin-2-dependent of myelin basic protein-specific T cells. Immunology. 2010; 130:114–24. [PubMed: 20059576]

[16]. Madsen LS, Andersson EC, Jansson L, Krogsgaard M, Andersen CB, Engberg J, et al. A humanized model for multiple sclerosis using HLA-DR2 and a human T-cell receptor. Nat Genet. 1999; 23:343–7. [PubMed: 10610182]

[17]. Beswick EJ, Reyes VE. CD74 in antigen presentation, inflammation and cancers of the gastrointestinal tract. World J Gastroenterol. 2009; 15:2855–61. [PubMed: 19533806]

[18]. Borghese F, Physician BM, Clanchy FIL. CD74: an emerging opportunity as a therapeutic target in cancer and autoimmune disease. Expert Opin Ther Targets. 2011; 15:237–51. [PubMed: 21208136]

[19]. Roche PA, Teletski CL, Stang E, Bakke O, Long EO. Cell surface HLA-DR-invariant chain complexes are targeted to endosomes by rapid internalization. Proc Natl Acad Sci U S A. 1993; 90:8581–5. [PubMed: 8397411]

[20]. Eynon EE, Schlax C, Pieters J. A secreted form of the major histocompatibility complex class II-associated invariant chain inhibiting T cell activation. J Biol Chem. 1999; 274:26266–71. [PubMed: 10473581]

[21]. Kudrin A, Scott M, Martin S, Chung C, Donn R, McMaster A, et al. Human macrophage migration inhibitory factor. J Biol Chem. 2006; 281:29641–51. [PubMed: 16893895]

[22]. Amin MA, Haas CS, Zhu K, Mansfield PJ, Kim MJ, Lackowski NP, et al. Migration inhibitory factor up-regulates vascular cell adhesion molecule-1 and inter-cellular adhesion molecule-1 via Src, PI3 kinase, and NF-kB. Blood. 2006; 107:2252–61. [PubMed: 16317091]

[23]. Fan H, Hall P, Santos LL, Gregory J, Fingerle-Rowson G, Bucala R, et al. Macrophage migration inhibitory factor and CD74 regulate macrophage chemotactic responses via MAPK and GFPase. J Immunol. 2011; 186:4915–24. [PubMed: 21411731]

[24]. Sinha S, Subramanian S, Proctor TM, Kaler LJ, Grafe M, Dahan R, et al. A promising therapeutic approach for multiple sclerosis: recombinant T-cell receptor ligands modulate experimental autoimmune encephalomyelitis by reducing interleukin-17 production and inhibiting migration of encephalitogenic cells into the CNS. J Neurosci. 2007; 27:12531–9. [PubMed: 18003831]

[25]. Sinha S, Subramanian S, Miller L, Proctor TM, Roberts C, Burrows GG, et al. Cytokine switch and bystander suppression of autoimmune responses to multiple antigens in experimental autoimmune encephalomyelitis by a single recombinant T-cell receptor ligand. J Neurosci. 2009; 29:3816–23. [PubMed: 19321778]

[26]. Sinha S, Subramanian S, Emerson-Webber A, Lindner M, Burrows GG, Grafe M, et al. Recombinant TCR ligand reverses clinical signs and CNS damage of EAE induced by recombinant human MOG. J Neuroimmune Pharmacol. 2010; 5:231–9. [PubMed: 19789980]

[27]. Watson K, Gooderham NJ, Davies DS, Edwards RJ. Nucleosomes bind to cell surface proteoglycans. J Biol Chem. 1999; 274:21707–13. [PubMed: 10419482]

[28]. Das R, Burke T, Plow EF. Histone H2B as a functionally important plasminogen receptor on macrophages. Blood. 2007; 110:3763–72. [PubMed: 17690254]

[29]. Das R, Plow EF. Phosphatidylserine as an anchor for plasminogen and its plasminogen receptor, histone H2B, to the macrophage surface. J Thromb Haemost. 2011; 9:339–49. [PubMed: 21040449]

[30]. Subramanian S, Zhang B, Kosaka Y, Burrows GG, Grafe MR, Vandenbark AA, et al. Recombinant T cell receptor ligand treats experimental stroke. Stroke. 2009 http://dx.doi.org/10.1161/STROKEAHA.108.543991.

[31]. Cresswell P. Invariant chain structure and MHC class II function. Cell. 1996; 84:505–7. [PubMed: 8598037]

[32]. Jasanoff A, Song S, Dinner AR, Wagner G, Wiley DC. One of two unstructured domains of Ii becomes ordered in complexes with MHC class II molecules. Immunity. 1999; 10:761–8. [PubMed: 10403651]

[33]. Lamb CA, Cresswell P. Assembly and transport properties of invariant chain trimers and HLA-DR-invariant chain complexes. J Immunol. 1992; 148:3478–82. [PubMed: 1588042]

[34]. Roche PA, Marks MS, Cresswell P. Formation of nine-subunit complex by HLA class II glycoproteins and the invariant chain. Nature. 1991; 354:392–4. [PubMed: 1956401]

[35]. Koch N, Zacharias M, Konig A, Temme S, Neumann J, Springer S. Stoichiometry of HLA class II-invariant chain oligomers. PLoS One. 2011; 6:e17257. [PubMed: 21364959]

[36]. Ashman JB, Miller J. A role for the transmembrane domain in the trimerization of the MHC class II-associated invariant chain. J Immunol. 1999; 163:2704–12. [PubMed: 10453012]

[37]. Castellino F, Han R, Germain RN. The transmembrane segment of invariant chain mediates binding to MHC class II molecules in a CLIP-independent manner. Eur J Immunol. 2001; 31:841–50. [PubMed: 11241289]

[38]. Dixon AM, Stanley BJ, Matthews EE, Dawson JP, Engelman DM. Invariant chain transmembrane domain trimerization: a step in MHC class II assembly. Biochem. 2006; 45:5228–34. [PubMed: 16618111]

[39]. King G, Dixon AM. Evidence for role of transmembrane helix-helix interactions in the assembly of the class II major histocompatibility complex. Mol Biosyst. 2010; 6:1650–61. [PubMed: 20379596]

[40]. Shi X, Leng L, Wang T, Wang W, Du X, Li J, et al. CD44 is the signaling component of the macrophage migration inhibitory factor-CD74 receptor complex. Immunity. 2006; 25:595–606. [PubMed: 17045821]

[41]. Bernhagen J, Krohn R, Lue H, Gregory JL, Zernecke A, Koenen RR, et al. MIF is a noncognate ligand of CXC chemokine receptors in inflammatory and atherogenic cell recruitment. Nat Med. 2007; 13:587–96. [PubMed: 17435771]

[42]. Leng L, Metz CN, Fang Y, Xu J, Donnelly S, Baugh J, et al. MIF signal transduction initiated by binding to CD74. J Exp Med. 2003; 197:1467–76. [PubMed: 12782713]

[43]. Naujokas MF, Morin M, Anderson MS, Peterson M, Miller J. The chondroitin sulfate form of invariant chain can enhance stimulation of T cell responses through interaction with CD44. Cell. 1993; 74:257–68. [PubMed: 8343954]

[44]. Denkinger CM, Denkinger M, Kort JJ, Metz C, Forsthuber TG. *In vivo* blockade of macrophage migration inhibitory factor ameliorates acute experimental autoimmune encephalomyelitis by impairing the homing of encephalitogenic T cells to the central nervous system. J Immunol. 2003; 170:1274–82. [PubMed: 12538686]

[45]. Powell ND, Papenfuss TL, McClain MA, Gienapp IE, Shawler TM, Satoskar AR, et al. Cutting edge: macrophage migration inhibitory factor is necessary for progression of experimental autoimmune encephalomyelitis. J Immunol. 2005; 175:5611–4. [PubMed: 16237048]

[46]. Binsky I, Lantner F, Grabovsky V, Harpaz N, Shvidel L, Berrebi A, et al. TAp63 regulates VLA-4 expression and chronic lymphocytic leukemia cell migration to the bone marrow in a CD74-dependent manner. J Immunol. 2010; 184:4761–9. [PubMed: 20357260]

[47]. Cheng Q, McKeown SJ, Santos L, Santiago FS, Khachigian LM, Morand EF, et al. Macrophage migration inhibitory factor increases leukocyte-endothelial interactions in human endothelial cells via promotion of expression of adhesion molecules. J Immunol. 2010; 185:1238–47. [PubMed: 20554956]

[48]. Nguyen K, Sylvain NR, Bunnell SC. T cell costimulation via the integrin VLA-4 inhibits the actin-dependent centralization of signaling microclusters containing the adaptor SLP-76. Immunity. 2008; 28:810–21. [PubMed: 18549800]

[49]. Katzman SD, O'Gorman WE, Villarino AV, Gallo E, Friedman RS, Krummel MF, et al. Duration of antigen receptor signaling determines T-cell tolerance or activation. Proc Natl Acad Sci U S A. 2010; 107:18085–90. [PubMed: 20921406]

[50]. Rohn TA, Boes M, Wolters D, Spindeldreher S, Muller B, Langen H, et al. Upregulation of the CLIP self peptide on mature dendritic cells antagonizes T helper type 1 polarization. Nat Immunol. 2004; 5:909–18. [PubMed: 15322540]

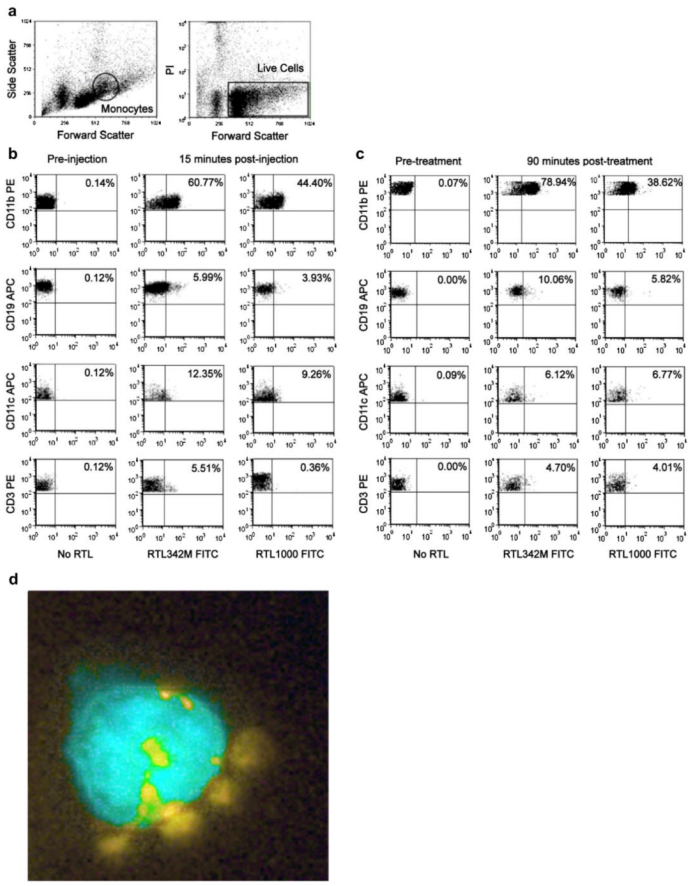

Fig. 1.

Binding of RTL constructs to PBMC (monocyte gate). Binding of RTL342M and RTL1000 to PBMC was analyzed on cell subtypes within the monocyte gate a) determined by excluding PI-positive (dead) cells and including only cells from the monocyte region as defined by forward and side scatter. b) Blood was collected *ex vivo* from naïve DR*1501-Tg mice 15 min after i.v. injection of 500 μg RTL342M (pDR2/mMOG-35-55)-FITC or RTL1000 (pDR2/hMOG-35-55)-FITC or c) labeled RTL342M and RTL1000 were incubated *in vitro* for 1hr at 37 °C with PBMC collected from naïve DR*1501-Tg mice. PBMC were counterstained for 30 min with fluorescent-labeled mAb specific for monocytes (CD11b), B-cells (CD19), dendritic cells (CD11c) and T-cells (CD3) prior to FACS evaluation. d) Isolated $GFP^{+}CD11b^{+}$ (color enhanced teal) cells from DR*1501/GFP-Tg mice were treated with 10 μg/ml RTL342M labeled with Alexa-546 (color enhanced yellow) for 40 min and evaluated by fluorescence microscopy. Data are representative of three independent experiments.

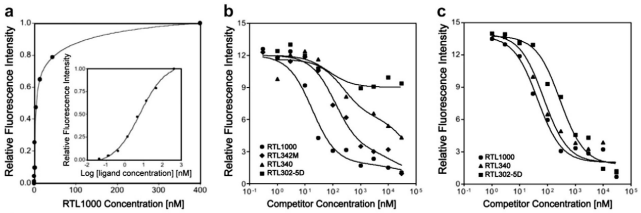

d

Competitor vs. RTL1000	DR*1501-Tg splenocytes EC50 (nM) (Site 1)	DR*1501-Tg splenocytes EC50 (nM) (Site 2)	MHC Class II deficient mouse splenocytes EC50 (nM)
RTL1000	4,000	11	71.1
RTL342M	14,900	122	ND
RTL340	87,000	140	43.2
RTL302-5D	NA	73	282

ND = Not Determined. NA = Not applicable

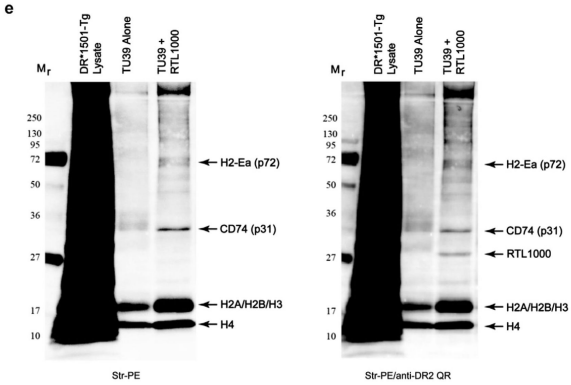

Fig. 2.

RTL1000 binding to splenocytes from DR*1501-Tg and MHC class II deficient mice. a) Naïve spleen cells (2×10^6) were incubated for 1 h on ice with increasing concentrations of AlexaFluor488-labeled RTL1000 (pDR2/hMOG-35-55). Instead of using RIPA buffer (which causes serious technical issues with whole cell solubilization), cells were lysed in 6 M urea to dissociate membrane-bound RTL for better analysis. After solubilization, samples were spun down to remove debris and proteins were separated by SDS electrophoresis in a 10–20%-PAGE and bands were quantified by densitometry by scanning the gel for Alexa488 fluorophore. The RTL1000 concentration (*X*-axis) was plotted against the fluorescence intensity (*Y*-axis). The data fit only the 2-binding site model, with an R^2 of 0.998, with relative affinities (K_D) of 2.65 nM and 131.0 nM, respectively. Competitive binding was evaluated for the RTL receptor on whole cells from DR*1501-Tg mice b) or MHC class II-KO splenocytes c), and the relative affinities (EC50) calculated for each competitor d). A two-site binding pattern was observed for all RTL constructs except "empty" RTL302-5D (DR2/no peptide) on splenocytes from DR*1501-Tg mice, and only a one-site binding pattern was observed for all constructs on splenocytes from MHC class II-KO mice. e) Immunoprecipitation of pDR2 binding proteins. To isolate membrane RTL1000 binding proteins, splenocytes from DR*1501-Tg mice were lysed with a CHAPS-containing buffer and TU39/RTL1000 complexes bound to Protein A beads were added to the lysate. Immune complexes were washed to remove unbound material and bound proteins were eluted by boiling in reducing electrophoresis sample buffer for 8–10 min. After elution, bound proteins were separated by SDS-PAGE and analyzed by Western blot, probed first with streptavidin-PE (left) and then with a Quantum-red anti-DR2 antibody, HK14 (right) and scanned to visualize the relevant chromophores. Arrows indicate protein bands that were bound by RTL1000 and RTL1000 itself.

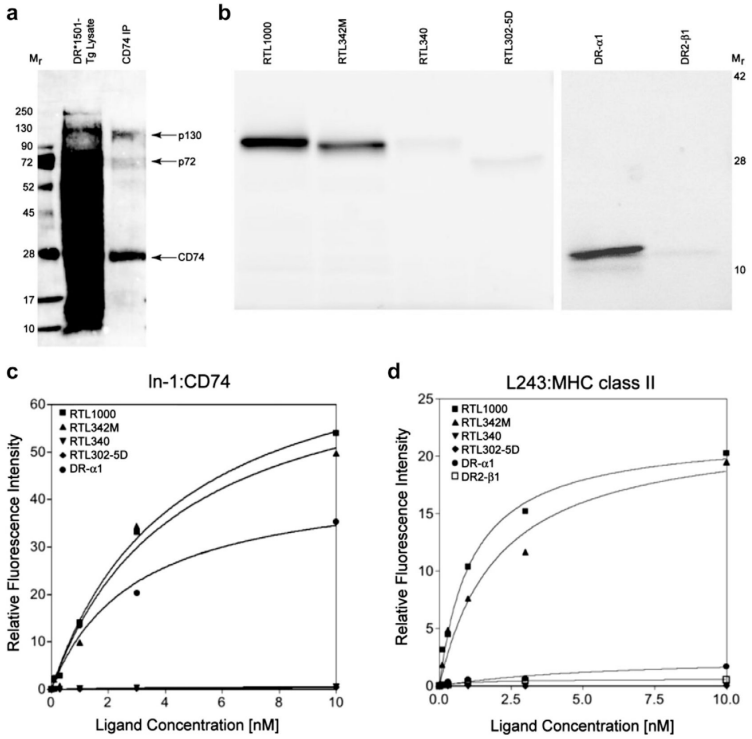

Fig. 3.

Binding of RTL constructs to immunopurified membrane CD74 and MHC class II. a) The lysate from membrane-biotinylated splenocytes from DR*1501-Tg mice was mixed with ln-1 bound to Protein L beads overnight at 4 °C. Immune complexes were washed 3 times with 1% CHAPS in TEN buffer (50 mM TRIS, 2 mM EDTA and 150 mM NaCl, pH 7.4) and once with TEN buffer to remove free material. Bound proteins were eluted by boiling the immune complexes in electrophoresis sample buffer for 8e10 min followed by centrifugation. Samples were analyzed by SDS-PAGE followed by Western blot and proteins were visualized using streptavidin-conjugated PE. The membrane was scanned in a Molecular Imager FX (BioRad) for PE fluorescence. *M*: molecular weight markers; DR*1501-Tg Lys: total lysate; CD74 IP: immunoprecipitated CD74. b) To evaluate binding of other RTL constructs, CD74 protein complexes were immunoprecipitated from biotin-labeled DR*1501-Tg splenocytes using ln-1 adsorbed onto Protein L/beads and incubated overnight with 250 nmols of FITC-labeled RTL, FITC-DR-α1 or FITC-DR2-β1 domains. Beads were washed 3 times and bound fluorescent RTL components were eluted as described above and analyzed by SDS-electrophoresis in a 10–20% PAGE. Gels were directly scanned for FITC chromophore as mentioned for panel a) and band intensity was determined by densitometry in a Molecular Imager FX (BioRad) with the Quantity One Software. c) FITC-labeled-RTL1000 (DR2/hMOG-35-55), RTL342M (DR2/mMOG-35-55), RTL340 (DR2/MBP-85-99) and the DR-α1 domain binding to ln-1 immunoprecipitated CD74 or d) L243-immunoprecipitated MHC class II was analyzed as a function of their concentration. Band intensity was determined by densitometry as described above. To isolate MHC class II, lysates were first depleted of CD74 with ln-1 bound to Protein L/beads overnight at 4 °C and the supernatant was subjected to a second round of immunoprecipitation with anti-human class II L243 monoclonal antibody adsorbed to Protein L/beads. Data from densitometry were plotted as ligand concentration vs. fluorescence intensity and analyzed using the Prism Software for one- or two-site binding with $R^2 > 0.95$ for all bound RTL. Binding constants (K_D) of RTL constructs to CD74 and

MHC class II assessed in this experiment are presented in Supplementary Fig. 5. All FITC-labeled bands were detected in a Bio-Rad Imager FX scanner followed by quantification by densitometry using Quantity One Software. Data were normalized and plotted vs. the RTL concentration and the curve was fit to one-site or two-site competition models and binding constants determined using the Prism Software. The best fit was found with the one-site competition equation.

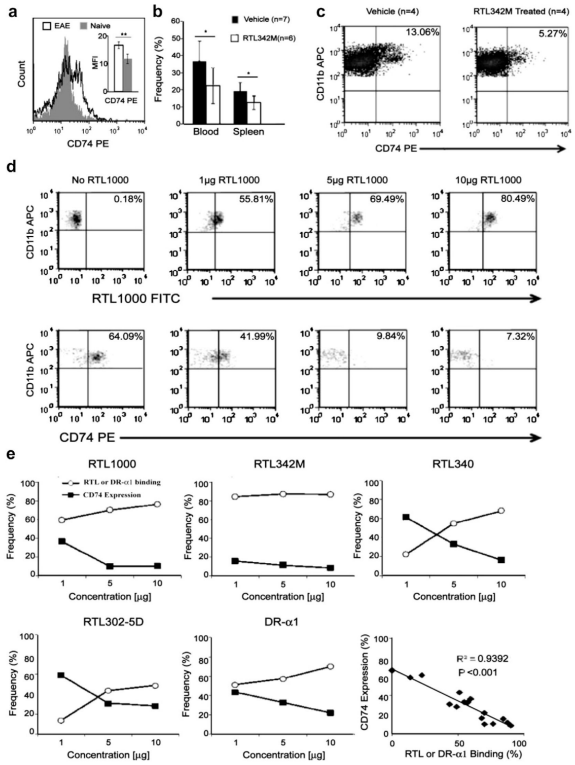

Fig. 4.

Dose-dependent downregulation of CD74 *in vivo* and *in vitro* by RTL constructs. a) Representative histogram and average mean fluorescence intensity (insert) of CD74 expression in blood monocytes from naïve ($n = 4$) and mMOG-35-55 immunized mice with EAE ($n = 4$)(**$p < 0.01$). CD74 expression in b) blood and spleen, and c) pooled spinal cords from DR*1501-Tg mice with EAE, 48 h after treatment with RTL342M (pDR2/mMOG-35-55) (100 μg) or vehicle (*$p < 0.05$). Mean EAE scores for mouse groups ($n = 4$) 48 h after treatment with vehicle or pDR2/mMOG-35-55 were 2.2 ± 0.5 vs. 1.6 ± 0.3, respectively ($p < 0.05$). d) Dot plots of RTL1000 (pDR2/hMOG-35-55)-FITC binding and CD74 expression of $CD11b^+$ monocytes. e) Dose-dependent binding of indicated RTL constructs (1 μg, 5 μg and 10 μg) *in vitro* with PBMC collected from naïve DR*1501-Tg mice. $CD11b^+$ monocytes were evaluated for RTL binding and CD74 expression by FACS. Bottom right panel: linear regression analysis of all constructs showing strong inverse correlation.

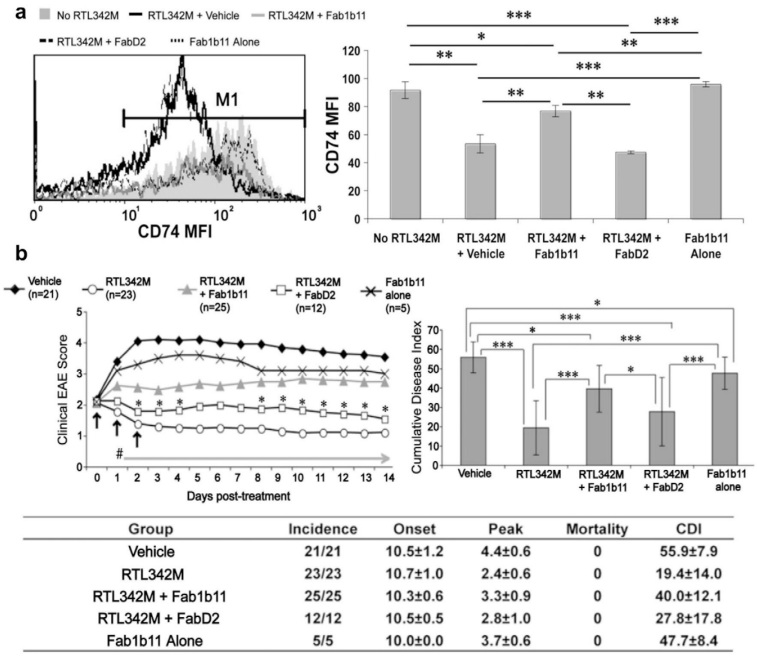

Group	Incidence	Onset	Peak	Mortality	CDI
Vehicle	21/21	10.5±1.2	4.4±0.6	0	55.9±7.9
RTL342M	23/23	10.7±1.0	2.4±0.6	0	19.4±14.0
RTL342M + Fab1b11	25/25	10.3±0.6	3.3±0.9	0	40.0±12.1
RTL342M + FabD2	12/12	10.5±0.5	2.8±1.0	0	27.8±17.8
Fab1b11 Alone	5/5	10.0±0.0	3.7±0.6	0	47.7±8.4

Fig. 5.

RTL-specific Fab blocks RTL342M-induced downregulation of CD74 expression on monocytes and neutralizes therapeutic activity in EAE. a) Fab1B11 specific for two-domain RTL342M (DR2/mMOG-35-55) but not FabD2 specific for a different RTL (DR4/GAD555-567) blocks binding to and expression of CD74 on $CD11b^+$ cells *in vitro* within the monocyte gate defined in Fig. 1a above in PBMC collected from naïve DR*1501-Tg mice. To neutralize RTL342M binding, 1 μg RTL was incubated at a 1:1 molar ratio (2 μg) of Fab1B11 or FabD2 for 2 h at room temperature prior to incubation with cells. Figure (left) shows mean fluorescent intensity (MFI) of CD74 after pre-incubation of RTL342M with Fab1B11 or control FabD2 or with no RTL or Fab1B11 alone. *$p < 0.05$; **$p < 0.005$; ***$p < 0.0005$. b) DR*1501-Tg mice with EAE were treated s.c. daily for 3 days at onset of clinical EAE with vehicle, 20 μg RTL342M alone, 20 μg RTL342M incubated for 2 h at a 1:1 (40 μg) or 1:2 molar ratio (80 μg) with Fab1B11 or 20 μg control FabD2 prior to injection or with 40 μg Fab1B11 alone. Top left: Daily mean clinical EAE disease scores. *$p < 0.05$, RTL342M + Fab1B11 vs. RTL342M + FabD2; #$p < 0.0005$, RTL342M vs. vehicle, RTL342M + Fab1B11 and Fab1B11 alone; RTL342M vs. RTL342M + FabD2 = ns. Top right: Statistical comparisons of cumulative disease indices (CDI): *$p < 0.05$; ***$p < 0.0001$. Bottom: Group EAE summary table. Daily mean scores were analyzed by Mann Whitney *U* and mean CDI by one way ANOVA with Tukey post-test, and nonparametric one way Kruskal–Wallis ANOVA with Dunn's multiple comparisons post-test.

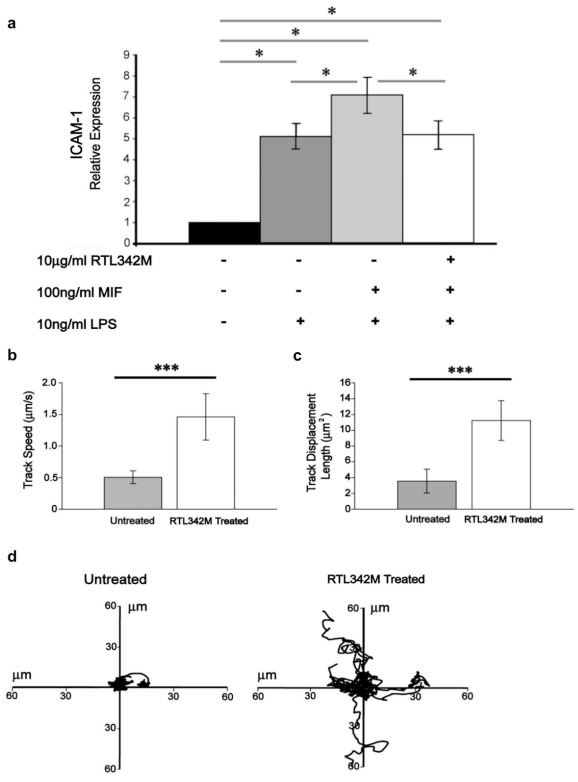

Fig. 6.

RTL binding to monocytes blocks MIF signaling and induces random migration. a) Splenocytes were isolated from 3 naïve DR*1501-Tg mice and treated with 10 µg/ml RTL342M (pDR2/mMOG-35-55) or buffer for 1 h, followed by 10 ng/ml LPS stimulation with or without 100 ng/ml MIF for 1 h and mRNA isolated. Relative expression of ICAM-1 was measured by real-time PCR (*$p < 0.05$). b–d) Isolated $GFP^{+}CD11b^{+}$ cells from DR*1501/GFP-Tg mice were treated with 50 µg/ml RTL342M for 2 h. Ten time-lapse fields (5 untreated and 5 RTL342M treated fields) were imaged by live fluorescence microscopy. b) Mean cell speed (micrometers per second) (***$p < 0.0005$). c) Mean track displacement length (square micrometers) (***$p < 0.0005$) of 10 fields. d) Tracks of individual cells (9–11 cells in each field) from four representative fields. Differences analyzed by Student's *T*-test.

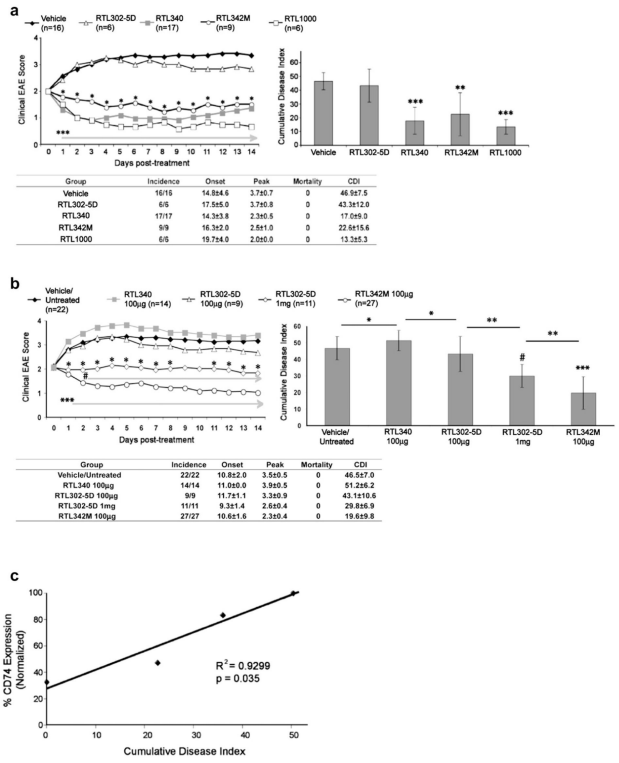

Fig. 7.

Potent downregulation of CD74 by RTL constructs enables bystander treatment of EAE. a) MBP-TCR/DR2-Tg mice with EAE were treated at disease onset with vehicle, RTL342M (DR2/mMOG-35-55), RTL1000 (DR2/hMOG-35-55), RTL340 (DR2/MBP-85-55) or "empty" RTL302-5D (DR2/no peptide). Mean clinical EAE daily disease scores (top left), cumulative disease index (top right), and group statistics summary table (bottom) are shown for each immunization group following 5 daily treatments. *$p < 0.02$, RTL342M vs. vehicle; ***$p < 0.002$, RTL340 and RTL1000 vs. vehicle (left panel). ***$p < 0.0001$ and **$p < 0.0014$ vs. vehicle (right panel). b) DR*1501 mice with EAE were untreated or treated at onset with vehicle (×2 or 5 daily treatments), RTL340 (100 μg × 5), RTL342M (100 μg × 2 or 5), "empty" RTL302-5D (100 μg × 5) and (1 μg × 2 or 5). Treatment data from vehicle vs. Untreated groups and groups receiving 2 vs. 5 daily treatments were not significantly different from each other and were combined. *$p < 0.05$, RTL302-5D (1 mg) vs. (100 μg); #$p < 0.03$, RTL302-5D (1 mg) vs. RTL342M (100 μg); ***$p < 0.0005$, RTL302-5D (1 mg) and RTL1000 (100 μg) vs. vehicle and RTL340 (left panel). #$p < 0.0001$, RTL302-5D (1 mg) vs. vehicle and RTL340; ***$p < 0.0001$, RTL342M (100 μg) vs. vehicle and RTL340 and RTL302-5D (100 μg); **$p < 0.004$; *$p < 0.05$ (right panel). Daily mean scores were analyzed by Mann Whitney *U* and mean CDI by one way ANOVA with Tukey post-test, and nonparametric one way Kruskal–Wallis ANOVA with Dunn's multiple comparisons post-test.